Irisin regulates thermogenesis and lipolysis in 3T3-L1 adipocytes

Maria Vliora[1,2], Elisabetta Grillo[2], Michela Corsini[2], Cosetta Ravelli[2], Eleni Nintou[1], Eleni Karligiotou[1], Andreas D. Flouris[1] and Stefania Mitola[2]

[1] FAME Laboratory, Department of Exercise Science, University of Thessaly, Trikala, Greece

[2] Department of Molecular and Translational Medicine, University of Brescia, Brescia, Italy

Corresponding authors: Stefania Mitola, stefania.mitola@unibs.it; Maria Vliora, mvliora@uth.gr

Abstract

Adipose tissue plays a pivotal role in the development and progression of the metabolic syndrome which along with its complications is an epidemic of the 21st century. Brown-like adipocytes reside within white adipose tissue (WAT) and respond to environmental cues releasing cytokines. Irisin is an adipo-myokine secreted mainly by skeletal muscle and targeting, among others, adipose tissue. In brown adipose tissue it upregulates uncoupling protein-1 (UCP1) which is responsible for mitochondrial non-shivering thermogenesis. Here we analysed the effects of irisin on the metabolic activity of 3T3-L1 derived adipocytes. Irisin affects mitochondrial respiration and lipolysis in a time-dependent manner through the regulation of PI3K-AKT pathway. Irisin also induces the expression of UCP1 and the regulation of NF-κB, and CREB and ERK pathways. Our data supports the role of irisin in the induction of non-shivering thermogenesis, the regulation of energy expenditure and lipolysis in adipocytes. Thus, irisin may be an attractive therapeutic target in the treatment of obesity and related metabolic disorders.

Keywords: browning, white adipose tissue, cell metabolism, signalling, mitochondrial respiration.

1. Introduction

Metabolic syndrome and its complications have become an epidemic in the twenty-first century and a major public health issue. Adipose tissue (AT) plays a pivotal role in the development and progression of the metabolic syndrome (Oladejo, 2011; Ordovas and Corella, 2008). AT is the most plastic organ in the human body and has the ability to constantly expand and regress (Granneman et al., 2005). It is the major organ that regulates energy homeostasis in living organisms and responds to environmental cues. Brown-like adipocytes reside within white adipose tissue (WAT) and can emerge through trans-differentiation after cold exposure, physical activity, and/or drug stimulation. This process is called browning of AT (Enerbäck, 2010; Valente et al., 2015b) and it is characterized by the increase of non-shivering thermogenesis, which depends on uncoupling protein 1 (UCP1) and increased lipolysis (Cannon and Nedergaard, 2004). Thus, AT browning leads to in heat production and/or energy dissipation and has been considered as a possible strategy for the treatment of obesity (di Somma et al., 2020).

Adipocytes play a central role in energy balance. Alteration of the mechanical, metabolic and secretory functions of adipocytes contribute to the pathogenesis of metabolic diseases, including obesity. For years, adipocytes were considered only as storage cells for triglycerides, with a passive role in the development of obesity. Today they are instead appreciated for their mechanical support, their thermal insulation function as well as the production of several hormone-like molecules, identified as adipokines (Langin, 2011; Shook et al., 2016). Notably, the release of adipokines changes, depending on

AT localization, on its cellular composition, and on the interaction with vascular structures as well as following the onset of obesity (Coelho et al., 2013).

Irisin is an adipo-myokine secreted mainly by skeletal muscle and by AT, after the proteolytic cleavage of fibronectin type III domain-containing protein 5 (FNDC5) (Boström et al., 2012). Physical activity induces the expression of irisin through the activation of the transcriptional factor peroxisome proliferator-activated receptor γ (PPARγ), the coactivator-1α (PGC-1α) and of FNDC5 (Dinas et al., 2021; Grygiel-Górniak and Puszczewicz, 2017). These pathways are involved in the browning of WAT (Zhang et al., 2016). The concentration of irisin into the bloodstream is also affected by diet and hormones, while its uptake and clearance are not yet well characterized (Korta et al., 2019).

The biological activity of irisin is not limited to adipocytes, since it can modulate several cellular responses, including proliferation, differentiation, and cell growth in normal and cancerous cells (Rabiee et al., 2020). Irisin binding to α-integrin receptor (Kim et al., 2018) activates the intracellular integrin-dependent signaling pathway, including the phosphorylation of focal adhesion kinase (FAK), extracellular signal-regulated kinases (ERK and MAPK), and the activator of transcription 3 (STAT3) in several cells including cardiomyocytes, hippocampal neuronal cells, and osteoblasts (Emanuele et al., 2014; Moon et al., 2013; Qiao et al., 2016). Moreover, irisin is involved in whole-body metabolism and thermoregulation by affecting thyroid hormone secretion (Raschke and Eckel, 2013; Valente et al., 2015a). In brown adipose tissue (BAT), it upregulates the expression of PGC-1a, leading to increased UCP1 expression and mitochondrial respiration (Fernandez-Marcos and Auwerx, 2011).

UCP1 expression leads to non-shivering thermogenesis which takes place in the inner mitochondrial membrane of brown adipose tissue (BAT), WAT, and skeletal muscle (Valente et al., 2015a) and can constitute up to 5% of the basal metabolic rate (van Marken Lichtenbelt and Schrauwen, 2011). The mitochondrial expression of UCP1 separates the oxidative phosphorylation from ATP synthesis with energy being dissipated as heat, a process referred to as the mitochondrial proton leak (Cannon and Nedergaard, 2004; Carrillo and Flouris, 2011).

Despite the accumulating information about irisin, our knowledge of its mechanistic effects on adipocytes remains poor and limits our understanding of how the thermogenic process occurs after irisin release in the circulation. Here, we examine the role of hr-irisin on non-shivering thermogenesis and energy expenditure using the well-characterized 3T3-L1 derived adipocytes model (Ruiz-Ojeda et al., 2016). We also monitor the time-dependent effects of hr-irisin on mitochondrial respiration and characterize the metabolic signaling pathways and the lipolytic process modulated by irisin. Our findings set the basis for the potential use of irisin as a therapeutic target in combating obesity and related metabolic disorders.

2. Materials and Methods

2.1 Reagents

All reagents were of analytical grade. DMEM media and fetal calf serum were purchased from GIBCO Life Technologies (Grand Island, NY). Insulin, dexamethasone, 3-isobutyl-methyl-xanthine, Oil Red O, EtOH Triton-X100, BriJ, and protease inhibitor were purchased from Sigma-Aldrich (St. Louis,

MO). Recombinant human irisin was purchased from (Cayman Chemical, Michigan, USA). Anti-phospho-NF-κB [sc101748; working dilution (wd) 1:1000], anti-NF-κB (sc109, wd 1:1000), anti-AKT (sc 1619, wd 1:1000), anti UCP- (sc 6529, wd 1:1000), anti-CREB (sc 186, wd 1:1000) antibodies were purchased from Santa Cruz Biotechnology (Santa Cruz, CA). Anti-ERK1,2 (#4695, wd 1:2000), anti-phospho-AKT (#4060, wd 1:2000) and anti-phospho-ERK1/2 (#4370, wd 1:2000) antibodies were purchased from Cell Signaling Technology (Beverly, MA). Donkey HRP-labeled secondary antibodies (anti-mouse Cat #SA1-100, wd 1:5000; anti rabbit Cat #31458, wd 1:5000; anti goat Cat #A16005, wd 1:5000) were purchased from Thermo Fisher Scientific.

2.2 Cell lines

Murine 3T3-L1 fibroblasts (ATCC, Manassas, VA) were maintained at no higher than 90% confluence in DMEM with 10% Bovine Serum (BS) and antibiotics (preadipocyte medium). To induce adipocyte differentiation, cell lines reaching the confluence received a differentiating medium, consisting of DMEM supplemented with 10% fetal bovine serum (FBS), 10 µg/ml insulin, 1 µM dexamethasone and 0.5 mM 3-isobutyl-methyl-xanthine (IBMX), for two days. The medium was then changed to 10% FBS-DMEM containing 10 µg/mL insulin. After the course of three to five days, differentiated adipocytes could be observed under the light microscope (accumulated lipid droplets in the cytoplasm) until day 12 to 15 of differentiation.

2.3 Oil Red O staining

Staining with Oil Red O was performed to confirm the differentiation of 3T3-L1 cells. On day 12 of differentiation the cell monolayer was fixed for 24-hours (h) with phosphate buffered formalin (10%). After rinsing with water and EtOH 70%, the monolayer was stained with the Oil Red O solution (water-based solution of 60% saturated Oil Red O in isopropanol) for 15-min. Excess stain was removed with EtOH 70% followed by a last wash with water before observation under an inverted photomicroscope (Zeiss, Axiovert 200M).

2.4 Extracellular mitochondrial flux assay

3T3-L1 preadipocytes were seeded on Seahorse XFe24 culture plates (Agilent, Santa Clara, CA, USA) in a density of 30,000 cells/well and differentiated into mature adipocytes as described above. Then, cells were treated with 20 nM hr-irisin (Boström et al., 2012) (Cayman Chemical, Michigan, USA) for 2-h and 4-h. Oxygen consumption rate (OCR) and extracellular acidification rate (ECAR) measurements were performed at 9-min intervals (3-min mixing, 3-min waiting and 3-min measuring) using a Seahorse XFe24 Extracellular Flux Analyzer (XFe Wave software) (Grillo et al., 2021). Seahorse XF Mito-Stress Test (Agilent, # 103015-100) was used to measure key parameters of mitochondrial function. Sequential treatments with oligomycin (1 µM), FCCP (0.5 µM) and rotenone/antimycin A (0.5 µM) were performed to enable quantification of basal OCR, ATP-coupled OCR, proton leak, and maximal respiration. Finally, cells were lysed and total proteins quantified by Bradford assay. Results are expressed as pmol of OCR / min for µg of proteins.

2.5 ATP measurement

ATP quantification was performed on $1x10^3$ cells in growth medium with ATP Determination Kit (Molecular Probes, Thermo Fisher Scientific, #A22066) following manufacturer's instructions. The bioluminescent signal was measured with EnSight Multimode Plate Reader (PerkinElmer, Waltham, Massachusetts, United States).

2.6 RT-qPCR

Total RNA was extracted using TRIzol Reagent (Invitrogen, Thermo Fisher Scientific) according to the manufacturer's instructions. Two µg of total RNA were retro-transcribed with MMLV reverse transcriptase (Invitrogen, Thermo Fisher Scientific) using random hexaprimers. Then, cDNA was analyzed by quantitative PCR using the following primers:

Plin1_For_TTACCTAGCTGCTTTCTCGGTG,
Plin1_Rev_CACAGGCAGCTGCAGAACTC;
Lipe_For_GCTGGGCTGTCAAGCACTGT,
Lipe_Rev_GTAACTGGGTAGGCTGCCAT;
ATGL_For_ACAGGGCTACAGAGATGGACT,
ATGL_Rev_AGGCTGCAATTGATCCTCCTC;
mGAPDH_For_CATGGCCTTCCGTGTTCCTAC,
mGAPDH_Rev_TTGCTGTTGAAGTCGCAGGAG.
mUCP1_For_AGGCTTCCAGTACCATTAGGT,
mUCP1_Rev_CTGAGTGAGGCAAAGCTGATTT.

Quantitative RT-PCR was performed using the iTaqTM Universal SYBR® Green Supermix (Bio-Rad, Hercules, CA, USA), by ViiA7 Real-Time PCR System (Life Technologies), and data were analyzed with Viia7 Real-Time Software (Life Technologies). 2-ΔΔCt was calculated using murine_GAPDH as housekeeping. Data are expressed as relative expression ratios. All samples were analysed in triplicates.

2.7 Western Blot

Whole-cell lysates were prepared in lysis buffer containing 1% Triton-X100, 0.1 BriJ, 1mM sodium orthovanadate, and protease inhibitor cocktail. 50 µg of total proteins were separated by SDS-PAGE and probed with specific antibodies and donkey HRP-labeled secondary antibodies. Chemiluminescent signal was acquired by ChemiDoc Imaging System (BioRad). All experiments were been performed in duplicates.

2.8 Statistical analysis

Statistical analysis was performed using SPSS 22.0 (IBM, Armonk, NY, USA). Paired samples t-tests were used to assess the differences in proton leak, basal OCR and mean ATP production. Repeated measures ANOVA was performed to assess differences in protein expression, gene expression, and ATP production. Post-hoc tests incorporating Bonferroni adjustment were performed for multiple comparisons. All values are reported as mean±SD. The level of significance was set at $p<0.05$.

3. Results

3.1 3T3-L1 differentiated cells show higher cellular respiration

In a first set of experiments, we differentiated murine 3T3-L1 cells into adipose cells and analysed their metabolic potential. To this, confluent cells were treated with differentiating medium for 12 days. As show in Figure 1A-C, the morphological changes of differentiated 3T3-L1 cells are clearly visible. These cells are filled with lipid droplets (Oil red O stained) visible under the microscope (Figure 1C).

Seahorse Mito-Stress Test was employed to measure key parameters of mitochondrial function, including basal respiration, ATP-linked respiration, spare capacity, proton leak, and maximal respiration by directly measuring the OCR of undifferentiated and 3T3-L1 derived adipocytes (Figure 1D-J). As expected, differentiation induced an increase in the metabolic capacity of 3T3-L1 cells as demonstrated by the significantly higher basal OCR (Figure 1E) and a simultaneous increase of the ECAR. Differentiation also significantly increased the maximal mitochondrial potential as demonstrated by the higher OCR measured upon treatment with the uncoupling agent FCCP (Figure 1H) and the proton leak (Figure 1G). These results confirm that our protocol was suitable to drive 3T3-L1 cell differentiation into mature adipocytes.

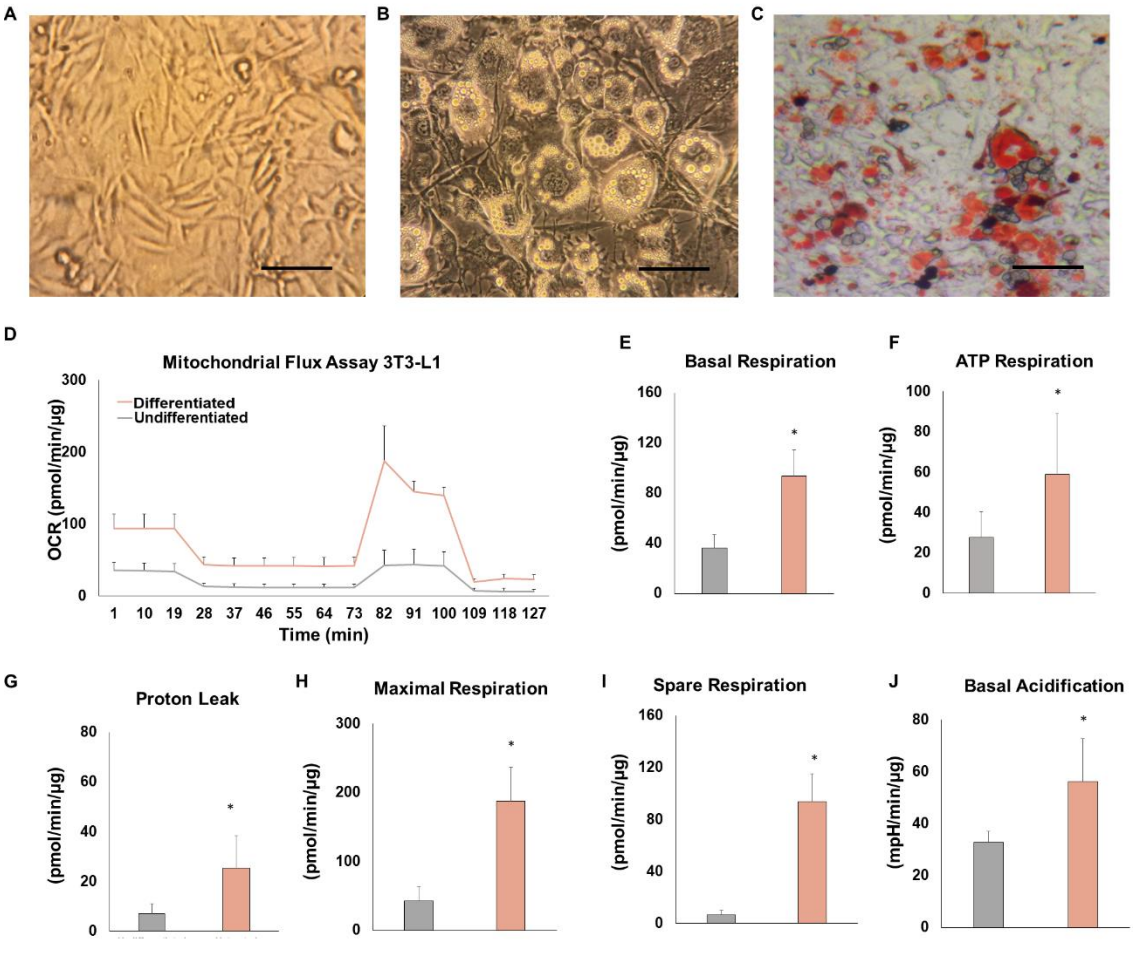

Figure 1. The differentiation of 3T3-L1 cells into adipose cells increases their mitochondrial metabolism. A-B) Representative images of undifferentiated (A) and differentiated 3T3-L1 cells (B) stuffed with lipid droplets (scale bar 20µm). **C**) Lipid droplets stained with oil O Red (scale bar 20µm). **D)** Seahorse Mito Stress Test performed on undifferentiated and differentiated 3T3-L1 cells. Sequential treatments with Oligomycin, FCCP and Rotenone/Antimycin A were performed to enable quantification of **E)** basal respiration, **F)** ATP-linked respiration, **G)** proton leak, **H)** maximal respiration, **I)** spare respiration and **J)** basal ECAR. Data were analyzed according to the Agilent Seahorse XF Cell Mito Stress Test Report Generator. * indicates statistically significant differences ($p<0.05$). Experiments were performed in triplicates.

3.2 Irisin regulates browning of 3T3-L1 derived adipocytes through PI3K-Akt pathway

To understand the effects of irisin on 3T3-L1 derived adipocytes, cells were treated for different times with 20 nM of hr-irisin. Then, 50 μg of the whole lysate were assessed for the activated intracellular signaling (Figure 2). Irisin rapidly increased the phosphorylation level of the transcriptional factor cAMP response element-binding protein (CREB) (Figure 2B), while nuclear factor kappa-light-chain-enhancer of activated B cells (NF-κB) (Figure 2C) was downregulated. Also, the activation of their upstream modulators including protein kinase B (AKT) and extracellular regulated kinase (ERK), were reduced after the treatment with irisin (Figure 2D-E). Irisin treatment induced a fast and transitory increase of the expression of the brown adipogenic marker UCP1 both at mRNA and protein levels (Figure 2F-G and S1), supporting the role of irisin in thermogenesis. Furthermore, the prolongation of irisin stimulation restored the UCP1 expression in 3T3-L1-derived adipocytes (Figure S1).

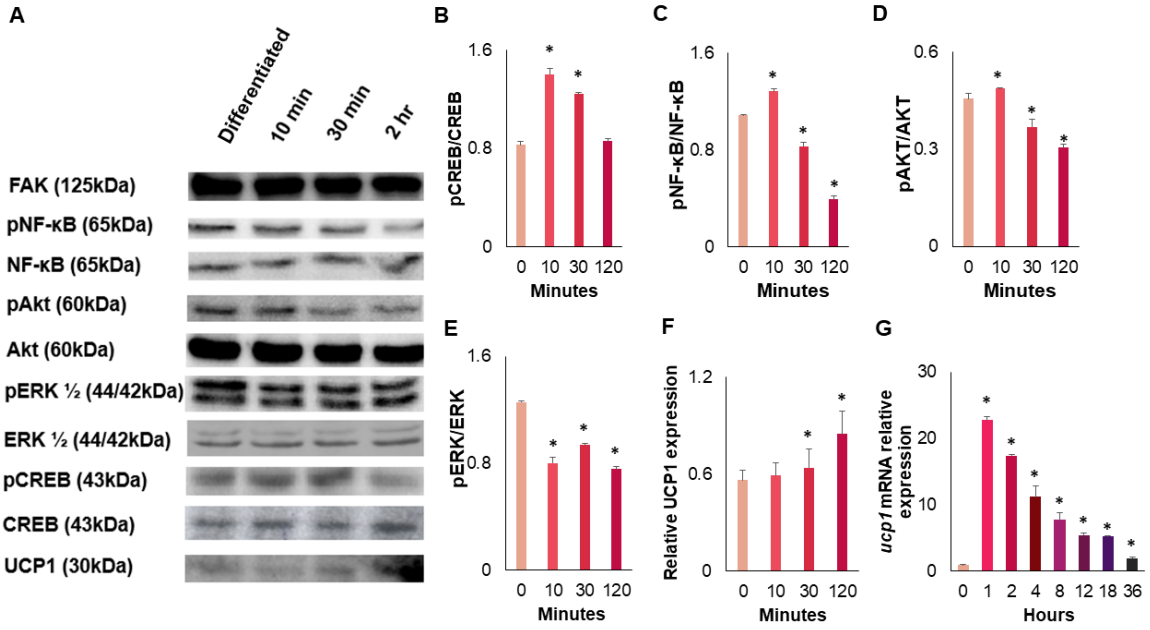

Figure 2. Irisin downstream effect on protein expression. **A)** Western blot analysis of 50µg of total protein lysates (all experiments were performed in duplicates). **B-E)** Phosphorylated vs unphosphorylated relative ratios for pCREB/CREB, pNF-κB/NF-κB, pAKT/AKT, and pERK/ERK were calculated by WB densitometry. **F)** Relative densitometric analysis of UCP1 protein normalized to FAK. **G)** mRNA expression of *ucp1* calculated by RT-qPCR. * indicates statistically significant differences ($p<0.05$) from untreated cells.

3.3 Irisin modulates cellular thermogenesis by reducing cellular respiration

The effects of irisin on UCP1 expression prompted us to delve into the molecular mechanisms involved in the modulation of AT metabolism. To this, we analyzed the OCR, an index of OXPHOS, in 20 nM irisin-treated adipocytes by Seahorse Mito-Stress Test (Figure 3A). Results showed that irisin rapidly affected the adipocyte metabolism. Indeed, the basal OCR was significantly reduced in the first 2-h of treatment [53±19.3 vs. 110±51.2 pmol/min/µg of

untreated cells ($p<0.05$)] and returned to basal levels upon prolonged stimulation 74±7.6 pmol/min/μg (Figure 3A-D). Importantly, to this point the amount of irisin in cell supernatant did not change over the stimulation (Figure S2).

The energy map combining OCR with ECAR, a readout of cell glycolytic activity (Figure 3B) indicated that 2-h of treatment with irisin results in a more quiescent metabolic profile, suggesting that irisin suppresses ATP production. Again, the energy phenotype was partially rescued at 4-h of treatment (Figure 3A). Also, proton leak and ATP-linked respiration show the same rapid and transitory increase (Figure 3C-E). Accordingly, irisin stimulation induced the expression of lipogenic genes including adipose triglyceride lipase (ATGL) and of the hormone-sensitive lipase (HSL). Perilipin (Plin1) continued to increase until 24-h after irisin treatment (Figure 4A). The production of ATP increased after 1-h of irisin stimulation, reaching a peak within 3-h (Figure 4B). Of note, 20 nM of irisin ensured a stimulation with a large excess of soluble stimulus. Indeed, the amount of irisin in cell supernatant was almost constant during the experimental timeframe (Figure S2).

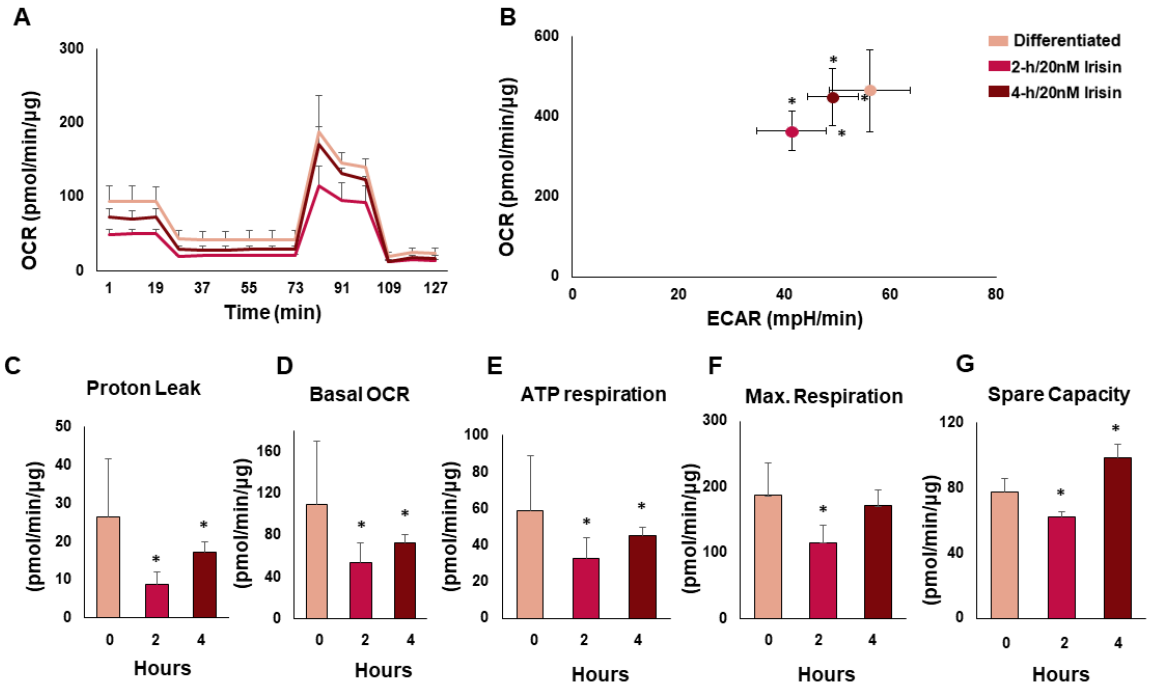

278

279 **Figure 3. Irisin reduces mitochondrial activity in adipose-derived 3T3 cells A**)
280 Seahorse Cell Mito Stress Test performed on adipose-derived 3T3 cells in the absence
281 or in the presence of 20 nM of irisin. Oxygen consumption rate (OCR) was recorded
282 over time before and after sequential addition of 1 µM oligomycin (Oligom), 0.5 µM
283 FCCP and 1 µM Rotenone/Antimycin-A (Rot/Anti-A). **B)** Stressed energy phenotype of
284 3T3-L1 differentiated adipocytes with different periods of treatment with hr-irisin.
285 Normalized OCR and ECAR were plotted to reveal overall basal metabolic profiles for
286 differently treated cells. **(C, D, E)** Proton leak, basal OCR and mean ATP-linked OCR
287 were calculated. Basal OCR was calculated by subtracting non-mitochondrial
288 respiration from baseline OCR. Note: * indicates statistical significance ($p<0.05$) from
289 untreated cells. Experiments were performed in triplicates.

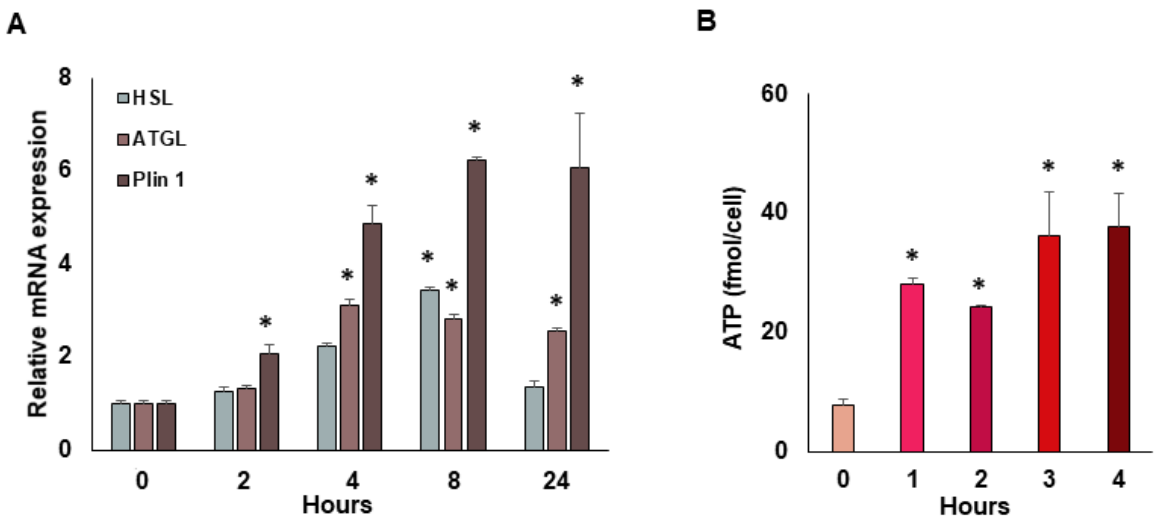

Figure 4. Irisin affects the expression of lipogenic genes A) Relative expression of HSL, ATGL and Plin1 during treatment with irisin (0-h to 24-h). **B)** ATP concentration at different time points during 4-h. * indicates statistically significant difference ($p<0.05$) from untreated cells. Experiments were performed in triplicates.

4. Discussion

Upon its discovery, irisin has been a subject of intense investigation (Dinas et al., 2021). Since irisin is an exercise-induced hormone (Boström et al., 2012) and passes a signal to AT, it is important to identify the molecular mechanisms that mediate its effects. Irisin holds an essential role in the upregulation of UCP1 (Arhire et al., 2019; Castillo-Quan, 2012; Zhang et al., 2016), which is abundant in the inner membrane of the BAT mitochondria. However, the mechanism through which irisin causes the upregulation of UCP1 remains unclear. Furthermore, the increase of irisin after physical exercise is another factor that needs to be clarified, since our current knowledge is based on measurements that took place across different time points, utilizing various exercise protocols (Boström et al., 2014). As a result, controversial data about the clearance of

irisin from the circulation exist in the literature. The present study addresses these gaps by defining a timeframe for the effect of irisin on adipocytes.

We found that irisin regulates *UCP1* gene in adipose derived 3T3-L1 cells inducing a fast and transitory increase in its expression, while it induces a slow and long-term upregulation of lipolytic genes. These data suggest that prolonged treatment with irisin could induce AT browning. Classically, *UCP1* gene expression is under the control of free fatty acids released upon extensive lipolysis (Fedorenko et al., 2012). However, more recent studies demonstrated that thermogenesis and *UCP1* expression is independent from lipolysis, suggesting that the two processes may be involved in AT browning through distinct mechanisms (Shin et al., 2018). Our results support this notion, showing that irisin induces a fast upregulation of *ucp1* gene that precedes, and is likely independent from, the upregulation of lipolytic genes. Moreover, we elucidated the intracellular signaling activated by irisin, which involves NF-κB (p65), AKT, pCREB, and pERK.

Adipocyte differentiation is under the control of PPARγ, which is responsible for regulating the expression of genes involved in adipogenesis and lipid storage (Boström et al., 2012; Rosen et al., 2000). PPARγ, which has an important role in adipocyte differentiation (Ahmadian et al., 2013), interacts with the p65 subunit of NF-κB by inhibiting NF-κB transcriptional activity (Chung et al., 2000). NF-κB is a physiological regulator of mitochondrial respiration (Mauro et al., 2011). We observed that phosphorylation of the p65 subunit of NF-κB, which enhances the selective NF-κB-mediated gene expression (Riedlinger et al., 2017), was attenuated at 30-min and 2-h of hr-irisin treatment (Figure 3B). The decreased phosphorylation of p65 after irisin administration in the medium

indicates that irisin induces adipocyte differentiation through the regulation NF-κB signaling pathway. The concomitant increase of UCP1 expression observed in this study further demonstrates the possible role of irisin in the induction of the browning process.

Irisin is involved in the molecular pathway that drives the expression of UCP1 which decreases the proton gradient developed in oxidative phosphorylation and generates heat (Ricquier, 2011). As revealed in our results, 2-h of irisin treatment on 3T3-L1 adipocytes moved the energy phenotype of the cells to a more quiescent state, indicating that the metabolic processes that produce energy in the form of ATP (oxidative phosphorylation and glycolysis) are initially restricted upon the presence of irisin. Of note, the ATP levels that we measured represent accumulated (produced and non-consumed) ATP in the cell medium. Accordingly, we found that accumulation of ATP in the medium increased after 1-h of irisin stimulation, reaching a peak within 3-h. Taken together, our findings suggest that during exercise, and consequent release of irisin, 3T3-L1 cells release ATP in the extracellular environment. This extracellular ATP could have an autocrine effect (e.g., on insulin stimulated glucose uptake) (Adamson et al., 2015) or be taken up by the muscle tissue as an extra fuel source (Fernández-Verdejo et al., 2014).

The quiescent state that the cells are transitioning to after irisin administration could also indicate a role of irisin on fatigue development. Here we examined the effects of irisin on adipocytes, but if the present results are also confirmed in muscle cells, this would suggest that irisin acts as an autocrine agent to induce fatigue, potentially as a protective mechanism. Also, it would be promising to use a systemic or an *in vitro* co-culture approach to

358 understand the cross-talk between the muscle and adipose tissues and its
359 potential role on fatigue development (Nintou et al., 2021).

360 AKT regulates glycolysis and oxidative phosphorylation in AT through
361 the glucose transporter (Altomare and Khaled, 2012), which mediates β3-
362 adrenergic signaling followed by increased lipolysis and glucose uptake
363 (Nonogaki, 2000). Our results are in line with previous findings demonstrating
364 that reduced AKT levels in AT can induce browning of WAT (Song et al., 2018).
365 Increased UCP1 expression accompanied by reduced activation of AKT upon
366 irisin stimulation indicates that irisin targets the PI3K-AKT pathway in AT. The
367 CREB is a downstream target of PI3K-AKT pathway (Peltier et al., 2007) and a
368 transcriptional regulator of UCP1 (Cao et al., 2004). CREB was activated
369 rapidly after irisin treatment, and its activation was present even after 2-h of
370 treatment. This confirms the involvement of irisin in UCP1 upregulation and its
371 role in thermogenesis. Accordingly, irisin induces the expression of lipolytic
372 genes, including ATGL, HSL and Plin1, which are necessary for thermogenesis.

373 Extracellular signal kinases (ERK ½) mediate an inhibitory effect of the
374 expression of UCP1 as a response to their phosphorylation of tumour necrosis
375 factor-alpha (TNF-α) (Valladares et al., 2001). During 2-h stimulation with irisin,
376 we observed that ERK ½ phosphorylation was reduced which indicates that
377 irisin may modulate TNF-α activity. As we did not directly measure the
378 expression of TNF-α, potential confirmation by future studies will demonstrate
379 the role of irisin in the browning of white adipocytes through ERK signaling.
380 Finally, we also measured the expression of FAK which participates in
381 adipocyte differentiation, and its disruption impairs adipocyte survival *in vitro* in
382 3T3-L1 adipocytes (Li and Xie, 2007; Luk et al., 2017). We did not observe

significant changes in the expression of FAK following irisin stimulation, indicating that it is not a molecular target of irisin in adipose tissue.

Following previous methodology (Boström et al., 2012), we treated our cells with 20 nM hr-irisin. This may be considered relatively high compared to the levels of irisin in human blood plasma reported in some studies. The literature data on circulating irisin levels are neither concordant nor conclusive, as the results depend on the affinity of the antibody used (Albrecht et al., 2015). Further analyses are necessary to establish the normative range of irisin in human blood plasma induced by physical activity (Albrecht et al., 2015). Therefore, we based our experimental design on the available literature of *in vitro* experiments (Boström et al., 2012), considering that *in vitro* experiments require higher concentrations of stimuli as there is no constant source of the cytokine as in the *in vivo* environment.

5. Conclusion

In summary, in this study we demonstrate that irisin regulates the mitochondrial respiration in 3T3-L1 derived adipocytes and exerts its effects 2-h after induction in the cellular environment. The effects of irisin occur through the following main pathways: (1) the partial depletion of the AKT signaling pathway, (2) the expression of lipolytic genes in adipocytes, as well as the upregulation of UCP1 through (3) the NF-κB signaling pathway, (4) the phosphorylation of CREB, and (5) the attenuation of ERK phosphorylation. Taken together, our findings demonstrate the potential role of irisin in the trans-differentiation of WAT, the induction of non-shivering thermogenesis and the regulation of

energy expenditure and lipolysis in adipocytes. Since AT metabolism holds a crucial role in combating obesity and related metabolic disorders, irisin can be an attractive therapeutic target that needs to be investigated in future studies.

Acknowledgments

This work received funding by H2020-MSCARISE- 2014 (Grant No. 645640 – SCAFFY). E.G. was funded by Fondazione Umberto Veronesi Fellowship.

Conflict of Interest Statement

The authors declare no conflict of interest.

Data Availability Statement

The datasets generated during and/or analyzed during the current study are available by the corresponding author on a reasonable request.

References

Adamson, S.E., A.K. Meher, Y.-h. Chiu, J.K. Sandilos, N.P. Oberholtzer, N.N. Walker, S.R. Hargett, S.A. Seaman, S.M. Peirce-Cottler, B.E. Isakson, C.A. McNamara, S.R. Keller, T.E. Harris, D.A. Bayliss, and N. Leitinger. 2015. Pannexin 1 is required for full activation of insulin-stimulated glucose uptake in adipocytes. *Molecular metabolism*. 4:610-618. doi: https://doi.org/10.1016/j.molmet.2015.06.009

Ahmadian, M., J.M. Suh, N. Hah, C. Liddle, A.R. Atkins, M. Downes, and R.M. Evans. 2013. PPARγ signaling and metabolism: the good, the bad and the future. *Nature medicine*. 19:557-566. doi: 10.1038/nm.3159

Albrecht, E., F. Norheim, B. Thiede, T. Holen, T. Ohashi, L. Schering, S. Lee, J. Brenmoehl, S. Thomas, C.A. Drevon, H.P. Erickson, and S. Maak. 2015. Irisin - a myth rather than an exercise-inducible myokine. *Scientific reports*. 5:8889-8889. doi: 10.1038/srep08889

Altomare, D.A., and A.R. Khaled. 2012. Homeostasis and the importance for a balance between AKT/mTOR activity and intracellular signaling. *Current medicinal chemistry*. 19:3748-3762. doi: 10.2174/092986712801661130

Arhire, L.I., L. Mihalache, and M. Covasa. 2019. Irisin: A Hope in Understanding and Managing Obesity and Metabolic Syndrome. *Frontiers in endocrinology*. 10:524. doi: 10.3389/fendo.2019.00524

Boström, P., J. Wu, M.P. Jedrychowski, A. Korde, L. Ye, J.C. Lo, K.A. Rasbach, E.A. Boström, J.H. Choi, J.Z. Long, S. Kajimura, M.C. Zingaretti, B.F. Vind, H. Tu, S. Cinti, K. Højlund, S.P. Gygi, and B.M. Spiegelman. 2012. A PGC1-α-dependent myokine that drives brown-fat-like development of white fat and thermogenesis. *Nature*. 481:463-468. doi: 10.1038/nature10777

Boström, P.A., J.M. Fernández-Real, and C. Mantzoros. 2014. Irisin in humans: recent advances and questions for future research. *Metabolism: clinical and experimental*. 63:178-180. doi: 10.1016/j.metabol.2013.11.009

Cannon, B., and J. Nedergaard. 2004. Brown adipose tissue: function and physiological significance. *Physiological reviews*. 84:277-359. doi: 10.1152/physrev.00015.2003

Cao, W., K.W. Daniel, J. Robidoux, P. Puigserver, A.V. Medvedev, X. Bai, L.M. Floering, B.M. Spiegelman, and S. Collins. 2004. p38 mitogen-activated protein kinase is the central regulator of cyclic AMP-dependent transcription of the brown fat uncoupling protein 1 gene. *Molecular and cellular biology*. 24:3057-3067. doi: 10.1128/mcb.24.7.3057-3067.2004

Carrillo, A.E., and A.D. Flouris. 2011. Caloric restriction and longevity: effects of reduced body temperature. *Ageing research reviews*. 10:153-162. doi: 10.1016/j.arr.2010.10.001

Castillo-Quan, J.I. 2012. From white to brown fat through the PGC-1α-dependent myokine irisin: implications for diabetes and obesity. *Disease models & mechanisms*. 5:293-295. doi: 10.1242/dmm.009894

Chung, S.W., B.Y. Kang, S.H. Kim, Y.K. Pak, D. Cho, G. Trinchieri, and T.S. Kim. 2000. Oxidized low density lipoprotein inhibits interleukin-12 production in lipopolysaccharide-activated mouse macrophages via direct interactions between peroxisome proliferator-activated receptor-gamma and nuclear factor-kappa B. *The Journal of biological chemistry*. 275:32681-32687. doi: 10.1074/jbc.M002577200

Coelho, M., T. Oliveira, and R. Fernandes. 2013. Biochemistry of adipose tissue: an endocrine organ. *Archives of medical science : AMS*. 9:191-200. doi: 10.5114/aoms.2013.33181

di Somma, M., M. Vliora, E. Grillo, B. Castro, E. Dakou, W. Schaafsma, J. Vanparijs, M. Corsini, C. Ravelli, E. Sakellariou, and S. Mitola. 2020. Role of VEGFs in metabolic disorders. *Angiogenesis*. 23:119-130. doi: 10.1007/s10456-019-09700-1

Dinas, P.C., A. Krase, E. Nintou, A. Georgakopoulos, M. Granzotto, M. Metaxas, E. Karachaliou, M. Rossato, R. Vettor, P. Georgoulias, T. S. Mayor, J. Koutsikos, K. Athanasiou, L.G. Ioannou, P. Gkiata, A.E. Carrillo, Y. Koutedakis, G.S. Metsios, A.Z. Jamurtas, S. Chatziioannou, and A.D. Flouris. 2021. Human white-fat thermogenesis: Experimental and meta-analytic findings. *Temperature*. 8:39-52. doi: 10.1080/23328940.2020.1769530

Emanuele, E., P. Minoretti, H. Pareja-Galeano, F. Sanchis-Gomar, N. Garatachea, and A. Lucia. 2014. Serum irisin levels, precocious myocardial infarction, and healthy exceptional longevity. *The American journal of medicine*. 127:888-890. doi: 10.1016/j.amjmed.2014.04.025

Enerbäck, S. 2010. Human Brown Adipose Tissue. *Cell metabolism*. 11:248-252. doi: https://doi.org/10.1016/j.cmet.2010.03.008

Fedorenko, A., P.V. Lishko, and Y. Kirichok. 2012. Mechanism of fatty-acid-dependent UCP1 uncoupling in brown fat mitochondria. *Cell*. 151:400-413. doi: 10.1016/j.cell.2012.09.010

Fernandez-Marcos, P.J., and J. Auwerx. 2011. Regulation of PGC-1α, a nodal regulator of mitochondrial biogenesis. *The American journal of clinical nutrition*. 93:884s-890. doi: 10.3945/ajcn.110.001917

Fernández-Verdejo, R., M. Casas, J.E. Galgani, E. Jaimovich, and S. Buvinic. 2014. Exercise sensitizes skeletal muscle to extracellular ATP for IL-6 expression in mice. *International journal of sports medicine*. 35:273-279. doi: 10.1055/s-0033-1353147

Granneman, J.G., P. Li, Z. Zhu, and Y. Lu. 2005. Metabolic and cellular plasticity in white adipose tissue I: effects of beta3-adrenergic receptor activation. *American journal of physiology. Endocrinology and metabolism*. 289:E608-616. doi: 10.1152/ajpendo.00009.2005

Grillo, E., M. Corsini, C. Ravelli, L. Zammataro, M. Bacci, A. Morandi, E. Monti, M. Presta, and S. Mitola. 2021. Expression of activated VEGFR2 by R1051Q mutation alters the energy metabolism of Sk-Mel-31 melanoma cells by increasing glutamine dependence. *Cancer Letters*. 507:80-88. doi: https://doi.org/10.1016/j.canlet.2021.03.007

Grygiel-Górniak, B., and M. Puszczewicz. 2017. A review on irisin, a new protagonist that mediates muscle-adipose-bone-neuron connectivity. *European review for medical and pharmacological sciences*. 21:4687-4693. doi:

Kim, H., C.D. Wrann, M. Jedrychowski, S. Vidoni, Y. Kitase, K. Nagano, C. Zhou, J. Chou, V.A. Parkman, S.J. Novick, T.S. Strutzenberg, B.D. Pascal, P.T. Le, D.J. Brooks, A.M. Roche, K.K. Gerber, L. Mattheis, W. Chen, H. Tu, M.L. Bouxsein, P.R. Griffin, R. Baron, C.J. Rosen, L.F. Bonewald, and B.M. Spiegelman. 2018. Irisin Mediates Effects on Bone and Fat via αV Integrin Receptors. *Cell*. 175:1756-1768.e1717. doi: 10.1016/j.cell.2018.10.025

Korta, P., E. Pocheć, and A. Mazur-Biały. 2019. Irisin as a Multifunctional Protein: Implications for Health and Certain Diseases. *Medicina (Kaunas, Lithuania)*. 55. doi: 10.3390/medicina55080485

Langin, D. 2011. In and Out: Adipose Tissue Lipid Turnover in Obesity and Dyslipidemia. *Cell metabolism*. 14:569-570. doi: https://doi.org/10.1016/j.cmet.2011.10.003

Li, J.J., and D. Xie. 2007. Cleavage of focal adhesion kinase (FAK) is essential in adipocyte differentiation. *Biochemical and biophysical research communications*. 357:648-654. doi: 10.1016/j.bbrc.2007.03.184

Luk, C.T., S.Y. Shi, E.P. Cai, T. Sivasubramaniyam, M. Krishnamurthy, J.J. Brunt, S.A. Schroer, D.A. Winer, and M. Woo. 2017. FAK signalling controls insulin sensitivity through regulation of adipocyte survival. *Nature communications*. 8:14360. doi: 10.1038/ncomms14360

Mauro, C., S.C. Leow, E. Anso, S. Rocha, A.K. Thotakura, L. Tornatore, M. Moretti, E. De Smaele, A.A. Beg, V. Tergaonkar, N.S. Chandel, and G. Franzoso. 2011. NF-κB controls energy homeostasis and metabolic adaptation by upregulating mitochondrial respiration. *Nature cell biology*. 13:1272-1279. doi: 10.1038/ncb2324

Moon, H.S., F. Dincer, and C.S. Mantzoros. 2013. Pharmacological concentrations of irisin increase cell proliferation without influencing markers of neurite outgrowth and synaptogenesis in mouse H19-7 hippocampal cell lines. *Metabolism: clinical and experimental*. 62:1131-1136. doi: 10.1016/j.metabol.2013.04.007

Nintou, E., E. Karligiotou, M. Vliora, I.G. Fatouros, A.Z. Jamurtas, N. Sakellaridis, K. Dimas, and A.D. Flouris. 2021. Effects of In Vitro Muscle Contraction on Thermogenic Protein Levels in Co-Cultured Adipocytes. *Life (Basel, Switzerland)*. 11. doi: 10.3390/life11111227

Nonogaki, K. 2000. New insights into sympathetic regulation of glucose and fat metabolism. *Diabetologia*. 43:533-549. doi: 10.1007/s001250051341

Oladejo, A.O. 2011. Overview of the metabolic syndrome; an emerging pandemic of public health significance. *Annals of Ibadan postgraduate medicine*. 9:78-82. doi:
Ordovas, J.M., and D. Corella. 2008. Metabolic syndrome pathophysiology: the role of adipose tissue. *Kidney international. Supplement*:S10-14. doi: 10.1038/ki.2008.517
Peltier, J., A. O'Neill, and D.V. Schaffer. 2007. PI3K/Akt and CREB regulate adult neural hippocampal progenitor proliferation and differentiation. *Developmental neurobiology*. 67:1348-1361. doi: 10.1002/dneu.20506
Qiao, X., Y. Nie, Y. Ma, Y. Chen, R. Cheng, W. Yin, Y. Hu, W. Xu, and L. Xu. 2016. Irisin promotes osteoblast proliferation and differentiation via activating the MAP kinase signaling pathways. *Scientific reports*. 6:18732. doi: 10.1038/srep18732
Rabiee, F., L. Lachinani, S. Ghaedi, M.H. Nasr-Esfahani, T.L. Megraw, and K. Ghaedi. 2020. New insights into the cellular activities of Fndc5/Irisin and its signaling pathways. *Cell & bioscience*. 10:51. doi: 10.1186/s13578-020-00413-3
Raschke, S., and J. Eckel. 2013. Adipo-myokines: two sides of the same coin--mediators of inflammation and mediators of exercise. *Mediators of inflammation*. 2013:320724. doi: 10.1155/2013/320724
Ricquier, D. 2011. Uncoupling protein 1 of brown adipocytes, the only uncoupler: a historical perspective. *Frontiers in endocrinology*. 2:85. doi: 10.3389/fendo.2011.00085
Riedlinger, T., M.B. Dommerholt, T. Wijshake, J.K. Kruit, N. Huijkman, D. Dekker, M. Koster, N. Kloosterhuis, D.P.Y. Koonen, A. de Bruin, D. Baker, M.H. Hofker, J. van Deursen, J.W. Jonker, M.L. Schmitz, and B. van de Sluis. 2017. NF-κB p65 serine 467 phosphorylation sensitizes mice to weight gain and TNFα-or diet-induced inflammation. *Biochimica et biophysica acta. Molecular cell research*. 1864:1785-1798. doi: 10.1016/j.bbamcr.2017.07.005
Rosen, E.D., C.J. Walkey, P. Puigserver, and B.M. Spiegelman. 2000. Transcriptional regulation of adipogenesis. *Genes & development*. 14:1293-1307. doi:
Ruiz-Ojeda, F.J., A.I. Rupérez, C. Gomez-Llorente, A. Gil, and C.M. Aguilera. 2016. Cell Models and Their Application for Studying Adipogenic Differentiation in Relation to Obesity: A Review. *International journal of molecular sciences*. 17. doi: 10.3390/ijms17071040
Shin, H., H. Shi, B. Xue, and L. Yu. 2018. What activates thermogenesis when lipid droplet lipolysis is absent in brown adipocytes? *Adipocyte*. 7:1-5. doi: 10.1080/21623945.2018.1453769
Shook, B., G. Rivera Gonzalez, S. Ebmeier, G. Grisotti, R. Zwick, and V. Horsley. 2016. The Role of Adipocytes in Tissue Regeneration and Stem Cell Niches. *Annu Rev Cell Dev Biol*. 32:609-631. doi: 10.1146/annurev-cellbio-111315-125426
Song, N.J., S.H. Chang, S. Kim, V. Panic, B.H. Jang, U.J. Yun, J.H. Choi, Z. Li, K.M. Park, J.H. Yoon, S. Kim, J.H. Yoo, J. Ling, K. Thomas, C.J. Villanueva, D.Y. Li, J.Y. Ahn, J.M. Ku, and K.W. Park. 2018. PI3Ka-Akt1-mediated Prdm4 induction in adipose tissue increases energy expenditure, inhibits weight gain, and improves insulin resistance in diet-induced obese mice. *Cell death & disease*. 9:876. doi: 10.1038/s41419-018-0904-3
Valente, A., A.E. Carrillo, M.N. Tzatzarakis, E. Vakonaki, A.M. Tsatsakis, G.P. Kenny, Y. Koutedakis, A.Z. Jamurtas, and A.D. Flouris. 2015a. The absorption and metabolism of a single L-menthol oral versus skin administration: Effects on thermogenesis and metabolic rate. *Food and chemical toxicology : an international journal published for the British Industrial Biological Research Association*. 86:262-273. doi: 10.1016/j.fct.2015.09.018
Valente, A., A.Z. Jamurtas, Y. Koutedakis, and A.D. Flouris. 2015b. Molecular pathways linking non-shivering thermogenesis and obesity: focusing on brown adipose tissue

development. *Biological reviews of the Cambridge Philosophical Society*. 90:77-88. doi: 10.1111/brv.12099

Valladares, A., C. Roncero, M. Benito, and A. Porras. 2001. TNF-alpha inhibits UCP-1 expression in brown adipocytes via ERKs. Opposite effect of p38MAPK. *FEBS letters*. 493:6-11. doi: 10.1016/s0014-5793(01)02264-5

van Marken Lichtenbelt, W.D., and P. Schrauwen. 2011. Implications of nonshivering thermogenesis for energy balance regulation in humans. *American journal of physiology. Regulatory, integrative and comparative physiology*. 301:R285-296. doi: 10.1152/ajpregu.00652.2010

Zhang, Y., C. Xie, H. Wang, R.M. Foss, M. Clare, E.V. George, S. Li, A. Katz, H. Cheng, Y. Ding, D. Tang, W.H. Reeves, and L.-J. Yang. 2016. Irisin exerts dual effects on browning and adipogenesis of human white adipocytes. *American Journal of Physiology-Endocrinology and Metabolism*. 311:E530-E541. doi: 10.1152/ajpendo.00094.2016

Figure legends

Graphical abstract. Intracellular pathways regulated by irisin in 3T3-L1 derived adipocytes.

Figure 1. The differentiation of 3T3-L1 cells into adipose cells increases their mitochondrial metabolism. A-B) Representative images of undifferentiated (A) and differentiated 3T3-L1 cells (B) stuffed with lipid droplets (scale bar 20µm). **C**) Lipid droplets stained with oil O Red (scale bar 20µm). **D)** Seahorse Mito Stress Test performed on undifferentiated and differentiated 3T3-L1 cells. Sequential treatments with Oligomycin, FCCP and Rotenone/Antimycin A were performed to enable quantification of **E)** basal respiration, **F)** ATP-linked respiration, **G)** proton leak, **H)** maximal respiration, **I)** spare respiration and **J)** basal ECAR. Data were analyzed according to the Agilent Seahorse XF Cell Mito Stress Test Report Generator. * indicates statistically significant differences ($p<0.05$). Experiments were performed in triplicates.

Figure 2. Irisin downstream effect on protein expression. **A)** Western blot analysis of 50µg of total protein lysates (all experiments were performed in duplicates). **B-E)** Phosphorylated vs unphosphorylated relative ratios for pCREB/CREB, pNF-κB/NF-κB, pAKT/AKT, and pERK/ERK were calculated by WB densitometry. **F)** Relative densitometric analysis of UCP1 protein normalized to FAK. **G)** mRNA expression of *ucp1* calculated by RT-qPCR. *

624 indicates statistically significant differences ($p<0.05$) from untreated cells.
625

626 **Figure 3. Irisin reduces mitochondrial activity in adipose-derived 3T3**
627 **cells A**) Seahorse Cell Mito Stress Test performed on adipose-derived 3T3
628 cells in the absence or in the presence of 20 nM of irisin. Oxygen consumption
629 rate (OCR) was recorded over time before and after sequential addition of 1 μM
630 oligomycin (Oligom), 0.5 μM FCCP and 1 μM Rotenone/Antimycin-A (Rot/Anti-
631 A). **B)** Stressed energy phenotype of 3T3-L1 differentiated adipocytes with
632 different periods of treatment with hr-irisin. Normalized OCR and ECAR were
633 plotted to reveal overall basal metabolic profiles for differently treated cells. **(C,**
634 **D, E)** Proton leak, basal OCR and mean ATP-linked OCR were calculated.
635 Basal OCR was calculated by subtracting non-mitochondrial respiration from
636 baseline OCR. Note: * indicates statistical significance ($p<0.05$) from untreated
637 cells. Experiments were performed in triplicates.

638

639 **Figure 4. Irisin affects the expression of lipogenic genes A)** Relative
640 expression of HSL, ATGL and Plin1 during treatment with irisin (0-h to 24-h).
641 **B)** ATP concentration at different time points during 4-h. * indicates statistically
642 significant difference ($p<0.05$) from untreated cells. Experiments were
643 performed in triplicates.